Carbohydrate Polymers 80 (2010) 474–479

Contents lists available at ScienceDirect

Carbohydrate Polymers

journal homepage: www.elsevier.com/locate/carbpol

Layer-by-layer structured polysaccharides film-coated cellulose nanofibrous mats for cell culture

Hongbing Deng [a,b], Xue Zhou [c], Xiaoying Wang [d], Chunyan Zhang [e], Bin Ding [b,e,*], Qiuhua Zhang [a], Yumin Du [a,*]

[a] School of Resource and Environmental Science, Wuhan University, Wuhan 430079, China
[b] State Key Laboratory for Modification of Chemical Fibers and Polymer Materials, Donghua University, Shanghai 201620, China
[c] Department of Environmental Medicine, School of Medicine, New York University, NY 10987, USA
[d] State Key Laboratory of Pulp and Paper Engineering, School of Light Industry and Food, South China University of Technology, Guangzhou 510640, China
[e] Nanomaterials Research Center, Modern Textile Institute, Donghua University, Shanghai 200051, China

ARTICLE INFO

Article history:
Received 23 October 2009
Received in revised form 2 December 2009
Accepted 3 December 2009
Available online 6 December 2009

Keywords:
LBL
Electrospinning
Polysaccharide
Cellulose nanofibrous mats
Cell culture

ABSTRACT

For the first time, a novel fibrous polysaccharide scaffold for cell culture was fabricated by the combination of electrospinning and electrostatic layer-by-layer (LBL) self-assembly technique. Oppositely charged chitosan (CS) and alginate (ALG) in aqueous media were alternatively deposited onto the negatively charged cellulose nanofibrous mats which hydrolyzed from electrospun cellulose acetate mats. The morphology and biocompatibility of the resultant scaffolds were investigated by regulating the pH of dipping solutions, the number of deposition bilayers, and the composition of outermost layer. Field emission scanning electron microscopy images indicated that the scaffolds possessed the fibrous structure and the thickness of CS/ALG bilayer formed on fibers was estimated in the range of 8–15 nm. The X-ray photoelectron spectroscopy results verified the existence of nitrogen element of CS on the surface of LBL films. The cell culture experiments demonstrated that the scaffolds have good biocompatibility for Beas-2B human bronchial epithelial cells in vitro.

1. Introduction

Functionallization of a solid surface by the electrostatic layer-by-layer (LBL) self-assembly technique introduced by Decher, Hong, and Schmitt (1992) has attracted considerable attention and became one of the most frequently utilized process for preparation of functional ultra-thin films (Ding, Fujimoto, & Shiratori, 2005a). The LBL self-assembly technique involves the step-wise and alternating adsorption of oppositely charged polyelectrolytes, particles, and ions on solid substrates with various shapes and sizes (Elbakry et al., 2009; Kim et al., 2007; Lee, Kim, Chen, Shao-Horn, & Hammond, 2009; Zhang, Chen, Sun, & Shen, 2007). Multilayers with well-defined thickness, composition, and structure at nanoscale precision can be easily fabricated from the aqueous media (Decher, 1997). Such LBL structured ultra-thin films have a broad range of applications including electrochromic devices (Laurent & Schlenoff, 1997), optical sensors (Lee, Kumar, & Tripathy, 2000), super-hydrophobic surfaces (Ogawa, Ding, Sone, & Shiratori, 2007), dye-sensitized solar cells (Kokubo, Ding, Naka, Tsuchihira, & Shiratori, 2007), etc.

Nanofibrous mats, obtained via electrospinning, possess some unique characteristics such as the ultra-thin fiber diameter, small pore size, high specific surface, three-dimensional (3D) structure, etc. (Ding, Kim, Kimura, & Shiratori, 2004b; Ding, Li, Fujita, & Shiratori, 2006b; Ji et al., 2006). The fibrous mats with negatively or positively charged fiber surface, low fiber density, and good water insolubility can be regarded as ideal templates for LBL deposition. Oppositely charged poly(acrylic acid) and anatase TiO_2 nanoparticles have been alternatively deposited on the cellulose acetate (CA) nanofibers and studied as a biomimetic super-hydrophobic surface and catalyst for decomposition of toxic gases (Ding, Kimura, Sato, Fujita, & Shiratori, 2004a). Additionally, Keggin-type polyoxometalate ($H_4SiW_{12}O_{40}$) nanotubes (Ding, Gong, Kim, & Shiratori, 2005b) were fabricated by calcination of LBL structured $H_4SiW_{12}O_{40}$/poly(allylamine hydrochloride) ultra-thin film-coated CA fibers. Although LBL deposition of these polyelectrolytes, nanoparticles and polyoxometalate on CA nanofiber templates was successful, this approach for deposition of polysaccharides on cellulose template fibers has never been done.

Encouraged by our recent progress (Kokubo et al., 2007; Ogawa et al., 2007) on the deposition of LBL films on electrospun nanofibers, we want to fabricate the wholly polysaccharide fibrous scaffolds for cell culture. Polysaccharides, chitosan (CS) and sodium alginate (ALG), can be used as starting materials to prepare stable

* Corresponding authors. Tel.: +86 21 62378202; fax: +86 21 62378392 (B. Ding), tel.: +86 27 68778501; fax: +86 27 68778501 (Y. Du).
E-mail addresses: binding@dhu.edu.cn (B. Ding), duyumin@whu.edu.cn (Y. Du).

0144-8617/$ - see front matter © 2009 Elsevier Ltd. All rights reserved.
doi:10.1016/j.carbpol.2009.12.004

LBL films. CS is one of the most abundant cationic polysaccharides in nature. The decisive driving force in the development of potential applications for CS due to the fact that CS is not only naturally abundant, but also nontoxic, biodegradable, and regenerated (Bhattarai, Edmondson, Veiseh, Matsen, & Zhang, 2005; Fakhry, Schneider, Zaharias, & Senel, 2004; Geng, Kwon, & Jang, 2005; Heinemann et al., 2009; Kurita, 2006; Ravi Kumar, 2000; Yi et al., 2005). In particular, it has been investigated that CS could preferentially promote the attachment and proliferation of cells (Heinemann, Heinemann, Bernhardt, Worch, & Hanke, 2008). ALG is another biodegradable polysaccharide derived from seaweed with the similar properties as CS such as non-toxicity, biocompatibility, biodegradability etc. and has been studied extensively attributing to the unique tissue compatibility and extensive applications in biomedicine (de Vos, Faas, Strand, & Calafiore, 2006; Lu, Zhu, Guo, Hu, & Yu, 2006; Sennerby, Röstiund, Albrektsson, & Albrektsson, 1987).

In this study, we have developed a straightforward and highly efficient method for the fabrication of the wholly polysaccharide fibrous scaffolds for cell culture via LBL self-assembly of CS and ALG on cellulose nanofibrous mats. The template fibrous cellulose mats can be hydrolyzed from the electrospun CA mats in alkaline solution. The influence of dipping solution pH and the number of coating bilayers on the formation of tubular LBL films deposited on cellulose nanofibers are investigated. Additionally, the cell culture experiments are carried out to examine the cellular compatibility of the prepared scaffolds.

2. Experimental details

The starting materials included cellulose acetate (CA, M_n 30,000, Aldrich Co., USA), sodium alginate (ALG, M_w 2.5×10^5, Aladdin Chemical Reagent Co., China), and chitosan (CS, M_w 2.1×10^5 KD, DD 92%, Yuhuan Ocean Biochemical Co., China). Acetone, *N*,*N*-dimethylacetamide (DMAC), acetic acid, sodium hydroxide, hydrogen chloride, and sodium chloride were supplied by Aladdin Chemical Reagent Co., China. All aqueous solutions were prepared using purified water with a resistance of 18.2 MΩ.

Nanofibrous CA mats were fabricated by electrospinning of a 15 wt.% CA solution prepared in a 2/1 (w/w) acetone/DMAc mixture. The CA solution was fed into a plastic syringe, which was driven by a syringe pump (LSP02-1B, Baoding Longer Precision Pump Co., Ltd., China). The positive electrode of a high voltage power supply (DW-P303-1ACD8, Tianjin Dongwen Co., China) was clamped to the metal needle tip of the syringe. A grounded cylindrical layer was used as a collector which rotated with a linear velocity of 100 m/min. The applied voltage was 16 kV and the tip-to-collector distance was 20 cm. The ambient temperature and relative humidity were maintained at 25 °C and 45%, respectively. The prepared fibrous mats were dried at 80 °C in vacuum for 24 h to remove the trace solvent. Hydrolysis of the CA mats was performed in a 0.05 M NaOH aqueous solution at ambient temperature for 7 days following the previous report (Ingrosso et al., 2006).

The LBL structured films were assembled on the cellulose nanofiber surface by alternating adsorption of positively charged CS and negatively charged ALG. The concentration of the CS solution was fixed as 1 mg/mL and its pH was controlled at 5. ALG solutions were prepared at the concentration of 1 mg/mL using pure water and their pH values were adjusted at 3, 4 and 5, respectively. The ionic strengths of CS, ALG, and rinsing solutions were regulated by adding NaCl at a 0.1 M concentration.

The concept for fabrication of fibrous polysaccharide scaffold is shown in Fig. 1. Firstly, nanofibrous cellulose mats were immersed into the CS solution for 20 min followed by 2 min of rising in three pure water baths. The mats then were immersed into ALG solution for 20 min followed by identical rinsing steps. The electrostatic adsorption and rinsing steps were repeated until the desired number of deposition layers was obtained. Herein, $(CS/ALGm)_n$ was referred to label the LBL structured films, where n was the number of the CS/ALG bilayers, m denoted the pH of ALG solution. The outermost layer was CS when n equaled to 5.5 and 10.5. All resultant samples were dried at 80 °C for 24 h in vacuum prior to the subsequent characterizations.

The morphology of samples was measured by field emission scanning electron microscopy (FE-SEM, S-4800, Hitachi Ltd., Japan). The diameters of the fibers were measured using an image analyzer (Adobe Photoshop 7.0). Fourier transform infrared (FT-IR) spectra were recorded using a Nicolet 170-SX instrument (Thermo Nicolet Ltd., USA). The surface elemental composition of samples was identified by X-ray photoelectron spectroscopy (XPS, Kratos Co., UK).

Beas-2B human bronchial epithelial cells were selected for the cellular compatibility experiments. The prepared scaffolds were cut into the size that can fit in the tissue culture plate, sterilized by UV light for 30 min, washed three times with phosphate buffered saline (PBS) solution, and then transferred to the culture plate. Beas-2B human bronchial epithelial cells (5×10^4) in 200 μL Dulbecco's Modified Eagle Medium (DMEM) were seeded onto the scaffold specimens in the culture plate. DMEM was supplemented with 10% fetal bovine serum (FBS) and 1% penicillin/streptomycin. Beas-2B cells grew at 37 °C in an incubator with a humidified atmosphere containing 5% CO_2. After 24 h, the samples were washed with PBS for three times to remove the unattached and dead cells, and then transferred to micro slides and mounted with ProLong Gold Anti-fade Reagent with DAPI (Molecular Probes Co., USA). The signals were visualized and captured by a Leica TSC SP5 confocal microscope.

3. Results and discussion

It is well known that the typical electrospun nanofibrous mats have a 3D structure with pores in micro and sub-micro size (Ding et al., 2005a). The deposition spaces among the adjacent fibers in

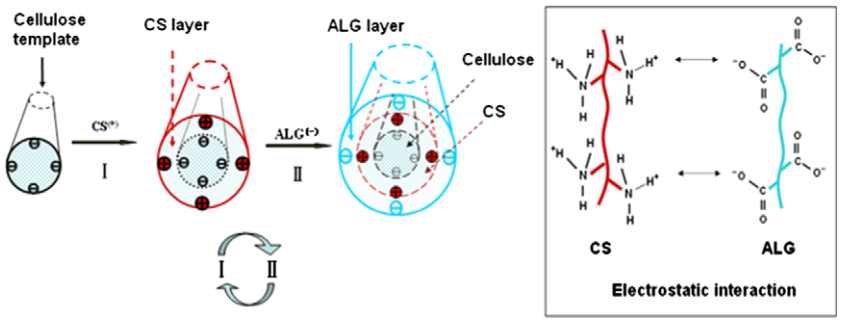

Fig. 1. Schematic diagram illustrating the fabrication of multi-layered CS/ALG films on cellulose nanofibers via electrostatic LBL deposition.

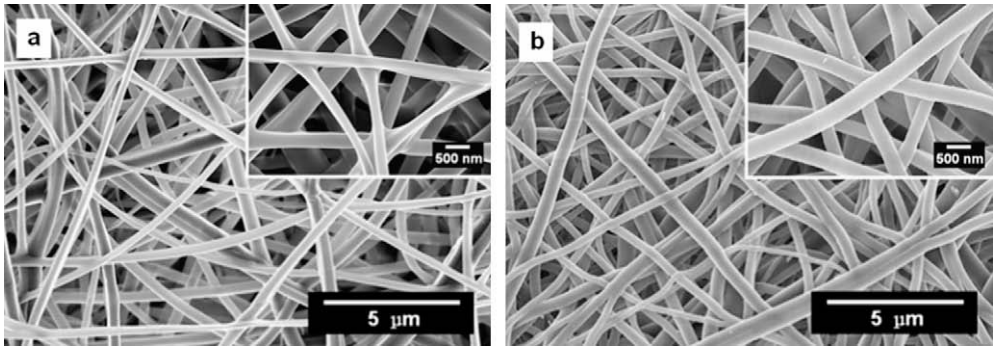

Fig. 2. FE-SEM images of fibrous CA (a) and cellulose (b) mats.

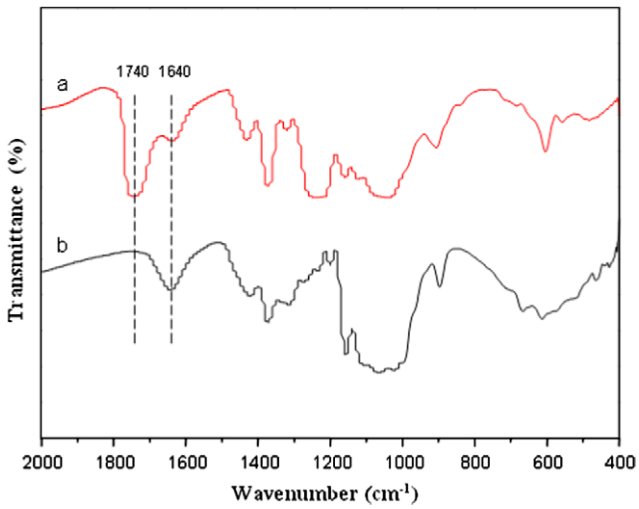

Fig. 3. FT-IR spectra of fibrous CA (a) and cellulose (b) mats.

nanofibrous mats are limited, which was different from the other flat substrates. Therefore, the optimization of the LBL deposition parameters is necessary for the fabrication of uniform LBL films on the surface of nanofibers.

Fig. 2a presents the FE-SEM image of as-spun CA mats. The CA mats were consisted of loosely packed cylindrical fibers with the average fiber diameter of 383 ± 134 nm. Some junctions were found among the CA fibers caused by the trace remained solvent after electrospinning. The FT-IR spectrum of CA mats is shown in Fig. 3a. The absorption features of CA were found at 1740 cm^{-1} (C═O) and 1640 cm^{-1} (C–O–O), respectively (Ding et al., 2004b). Additionally, the absorption peak at 1050 cm^{-1} was observed in case of the symmetrical C–O stretching. After alkaline hydrolysis, the fibers (Fig. 2b) were observably enlarged in width, bundled more closely, and merged together with other adjacent fibers along the fiber axis or around crossover junctions. The average diameter of hydrolyzed fibers was 405 ± 131 nm. The complete hydrolysis of CA fibers in mats was confirmed by the FT-IR result in Fig. 3b. The acetyl carbonyl (C═O) peak became indistinguishable which confirmed the conversion of all acetyl to hydroxyl.

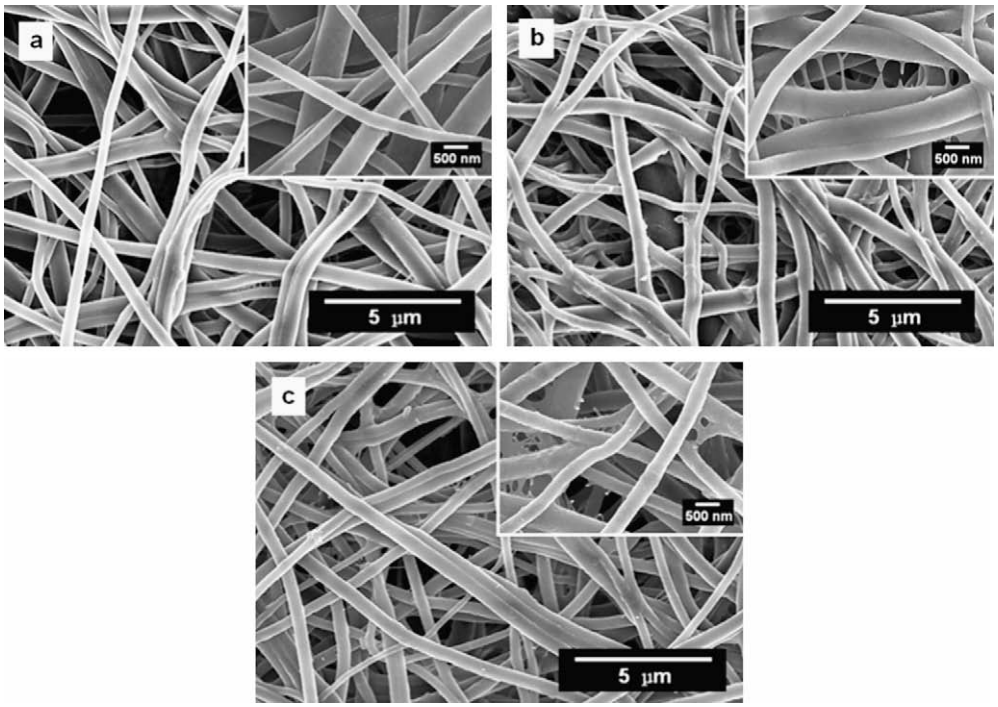

Fig. 4. FE-SEM images of $(CS/ALGm)_5$ films coated mats: (a) $m = 3$, (b) $m = 4$, and (c) $m = 5$.

Table 1
The characteristics of LBL films coated samples.

LBL films	Average fiber diameter (nm)	Standard deviation (nm)	Average film thickness (nm)	Average bilayer thickness (nm)
$(CS5/ALG3)_5$	456	147	51	10
$(CS5/ALG4)_5$	479	163	74	15
$(CS5/ALG5)_5$	430	131	25	5
$(CS5/ALG4)_{5.5}$	459	138	54	10
$(CS5/ALG4)_{10}$	486	147	83	8
$(CS5/ALG4)_{10.5}$	485	183	80	8

In general, the pH of dipping solutions plays an important role in the formation and morphology of LBL film-coated fibrous mats (Ding et al., 2005b). In order to determine the pH effect on the formation of LBL films on cellulose nanofibers, the pH values of ALG solutions were systematically regulated at 3, 4, and 5, respectively. Fig. 4 shows the morphology of the mats coated with LBL films forming with various pH values of ALG solutions. After the deposition of LBL films, the scaffolds still retained the nanofibrous 3D structure. Particularly, the average diameter of $(CS/ALGm)_5$ film-coated cellulose fibers (Fig. 4b) was increased from 405 nm (cellulose nanofibers) to 456 ($m = 3$), 479 ($m = 4$), and 430 ($m = 5$) nm (Table 1), respectively. The average thickness for each bilayer of the coated fibers could be estimated to 10 ($m = 3$), 15 ($m = 4$), and 5 ($m = 5$) nm, respectively. It can be seen that the LBL films grew fast on the cellulose fibers when the pH of ALG solution was 4. Additionally, several conglutinations between bundles of fibers were observed in Fig. 4b, which revealed that the LBL films formed between the adjacent fibers were splitted into webs during the drying process. In aqueous solution, pH is critical for the protonization of polyelectrolyte chains (Kim, Chung, Shin, Yam, & Chung, 2008). At the low pH of 4, the carboxyl groups of ALG were protonized and its negative charge would weakly interact with the positively charged amino groups of CS (Pasparakis & Bouropoulos, 2006), so the formation of the LBL structured CS/ALG films was sensitive to the pH of the dipping solutions.

To investigate the influence of the number of coating bilayers on the formation of LBL films coated nanofibers, the cellulose nanofibers were coated with various CS/ALG4 bilayers. The FE-SEM images of cellulose fibers coated with various bilayers of CS/ALG4 are shown in Figs. 4b and 5. There was no significant morphology difference between 5 and 5.5, or 10 and 10.5 bilayers coated mats. But doubling the bilayers showed thicker deposition as observed in FE-SEM images. Meanwhile, compared with the smooth surface of the cellulose fibers, the LBL film-coated samples showed a relatively high surface roughness on each fiber by forming some protuberances, which could be regarded as the irregular deposition of LBL films. The roughness on the fiber surface caused by the dispersion speed of deposition materials into the space-limited 3D structure of cellulose mats was different for the nanofibers distributed in the various sites (Ding, Li, Miyauchi, Kuwaki, & Shiratori, 2006a). Additionally, the surface layers were enriched in segments from the outermost layer. Once the next layer was deposited, it would interpenetrate into the previously adsorbed layer (Shiratori & Rubner, 2000).

XPS scans were used to verify the surface compositions of various resultant samples. Fig. 6 shows the XPS data of cellulose mats and $(CS/ALG4)_{10.5}$-coated samples. For cellulose mats (Fig. 6a), the carbon and oxygen peaks were observed with an oxygen:carbon ratio of 0.50:1. After the $(CS/ALG4)_{10.5}$ film deposition, a new nitrogen peak (N1s) at 400 eV was found in the XPS spectrum (Fig. 6b). Moreover, the surface layer of the LBL coated mats showed a oxygen:carbon:nitrogen ratio of 0.46:1:0.07. This result indicated the existence of CS in the samples after the LBL coating.

Beas-2B human bronchial epithelial cells were co-cultured with the resultant composite polysaccharide scaffolds in order to investigate their biocompatibility. For both in vitro and in vivo applications, materials are expected to possess their structural integrity in an aqueous environment (Bhattarai, Li, Edmondson, & Zhang, 2006). All scaffolds were fabricated in aqueous media retained the nanofibrous 3D structure throughout the LBL process. Preliminary observation from the images of Beas-2B cells collected by confocal microscope with 10× magnification (Fig. 7), the fibrous mats

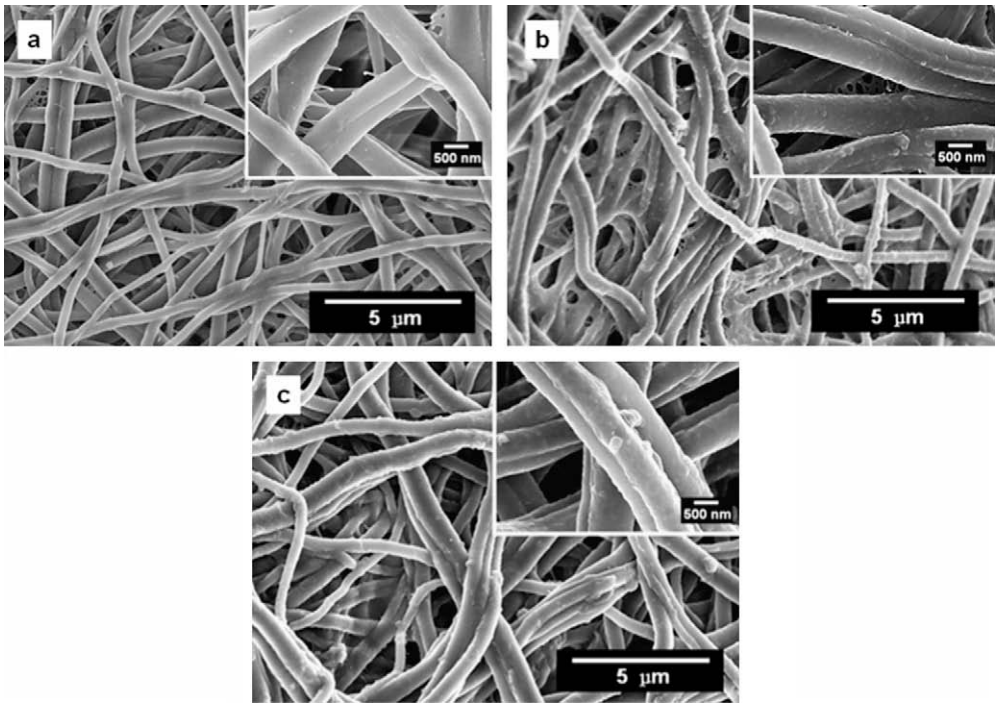

Fig. 5. FE-SEM images of $(CS/ALG4)_n$ films coated mats: (a) $n = 5.5$, (b) $n = 10$, and (c) $n = 10.5$.

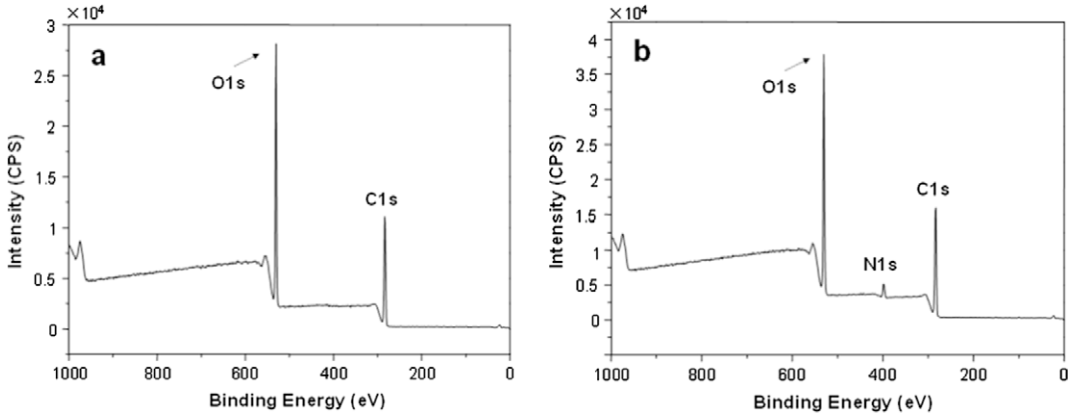

Fig. 6. XPS data taken from the nanofibrous mats of (a) cellulose and (b) $(CS/ALG4)_{10.5}$ film-coated cellulose.

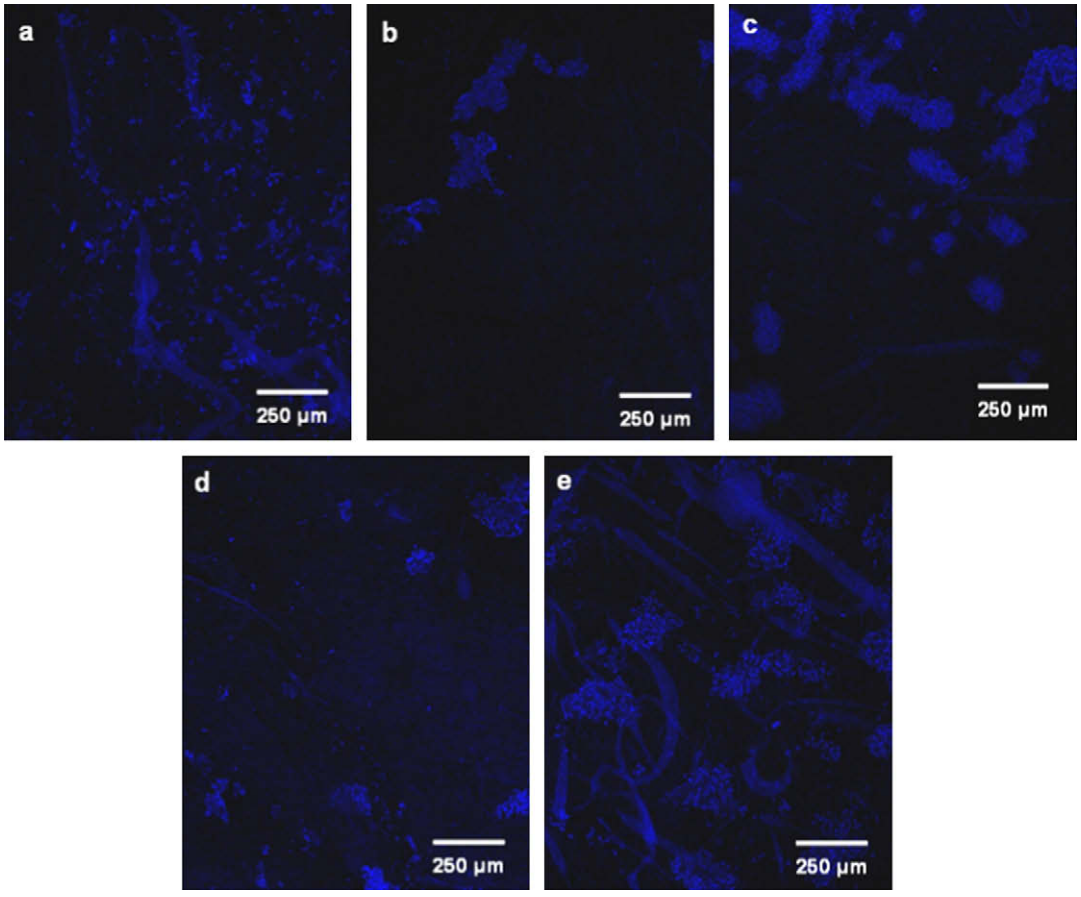

Fig. 7. Confocal microscope observation of cells cultured on scaffolds containing $(CS/ALG4)_n$ films for 24 h: (a) $n = 0$, (b) $n = 5$, (c) $n = 5.5$, (d) $n = 10$, and (e) $n = 10.5$.

could be perceived with the eyes directly and the novel scaffolds provided a suitable support for cell adhesion. Clearly, different cell morphologies were observed on various mats. Compared with the cellulose nanofibrous mats (Fig. 7a), Beas-2B cells showed polygonal morphology and formed cell clusters among the scaffolds (Fig. 7b–e). The cell morphology and attachment among the $(CS/ALG4)_n$ films coated mats changed remarkably while n varied from 5 to 10.5. The amount of adhesive cells on the scaffolds with the outermost layer of CS (Fig. 7c and e) was much larger than that of scaffolds with the outermost layer of ALG (Fig. 7b and d). The result was identical to the previous reports (Bhattarai et al., 2006; Rowley, Madlambayan, & Mooney, 1999) that the bulk ALG scaffolds usually require to be precoated with cell adhesive proteins such as fibronectin or arginine–glycine–aspartic acid peptides to promote cell adhesive ability.

Observed from Fig. 7, the scaffolds with the outermost layer of CS allowed the assembly of cells into 3D constructions with uniform cell clusters distribution. The promotion effect of CS on cell adhesion has been widely investigated (Yang, Chen, & Wang, 2009) and was explained by the cationic carried CS could attract the cells via electrostatic interaction (Yang et al., 2009). This result suggested that the outermost layer of LBL structured films would

affect the initial attachment of cells onto scaffolds. Additionally, for the scaffolds with the outermost layer of CS, the density of cell clusters was increased with increasing of the number of coating bilayers. So far, the underlying mechanism for such an enhancement in cell adhesion was not clear. Based on the FE-SEM results in Fig. 5, we found that the thickness of the LBL films and the average diameter of the fibers were proportional with the number of coating bilayers. Increasing the coating bilayers would provide a high binding site density for cells to enhance the cellular biocompatibility of scaffolds (Bhattarai et al., 2006; Zhang, Lim, Ramakrishna, & Huang, 2005).

4. Conclusions

Nanofibrous cellulose mats, used as polysaccharide template for LBL deposition, were successfully fabricated by electrospinning of CA solution with the subsequent alkaline hydrolysis treatment. The surface modification of cellulose mats with CS and ALG via the electrostatic LBL self-assembly technique to form a scaffold for cell culture. The various morphologies of fibrous scaffolds were obtained by regulating the pH of ALG solution and the number of coating bilayers. The results of cell culture experiments indicated that the biocompatibility of the prepared scaffolds was strongly affected by the composition of the outermost layer and the number of coating bilayers. The scaffold with the $(CS/ALG4)_{10.5}$ films exhibited the best good biocompatibility for Beas-2B cells.

Acknowledgments

This project was funded by the State Key Laboratory for Modification of Chemical Fibers and Polymer Materials, Donghua University, China. Partial support from the Program of Introducing Talents of Discipline to Universities (No. 111-2-04 and B07024) and the National Natural Science Foundation of China (No. 30972323) were appreciated.

References

Bhattarai, N., Edmondson, D., Veiseh, O., Matsen, F. A., & Zhang, M. (2005). Electrospun chitosan-based nanofibers and their cellular compatibility. *Biomaterials, 26*, 6176–6184.

Bhattarai, N., Li, Z. S., Edmondson, D., & Zhang, M. Q. (2006). Alginate-based nanofibrous scaffolds: Structural, mechanical, and biological properties. *Advanced Materials, 18*, 1463–1467.

de Vos, P., Faas, M. M., Strand, B., & Calafiore, R. (2006). Alginate-based microcapsules for immunoisolation of pancreatic islets. *Biomaterials, 27*, 5603–5617.

Decher, G. (1997). Fuzzy nanoassemblies: Toward layered polymeric multicomposites. *Science, 277*, 1232–1237.

Decher, G., Hong, J. D., & Schmitt, J. (1992). Buildup of ultrathin multilayer films by a self-assembly process. III: Consecutively alternating adsorption of anionic and cationic polyelectrolytes on charged surfaces. *Thin Solid Films, 210–11*, 831–835.

Ding, B., Fujimoto, K., & Shiratori, S. (2005a). Preparation and characterization of self-assembled polyelectrolyte multilayered films on electrospun nanofibers. *Thin Solid Films, 491*, 23–28.

Ding, B., Gong, J., Kim, J., & Shiratori, S. (2005b). Polyoxometalate nanotubes from layer-by-layer coating and thermal removal of electrospun nanofibres. *Nanotechnology, 16*, 785–790.

Ding, B., Kim, J., Kimura, E., & Shiratori, S. (2004b). Layer-by-layer structured films of TiO_2 nanoparticles and poly(acrylic acid) on electrospun nanofibres. *Nanotechnology, 15*, 913–917.

Ding, B., Kimura, E., Sato, T., Fujita, S., & Shiratori, S. (2004a). Fabrication of blend biodegradable nanofibrous nonwoven mats via multi-jet electrospinning. *Polymer, 45*, 1895–1902.

Ding, B., Li, C. R., Fujita, S., & Shiratori, S. (2006b). Layer-by-layer self-assembled tubular films containing polyoxometalate on electrospun nanofibers. *Colloids and Surfaces A – Physicochemical and Engineering Aspects, 284*, 257–262.

Ding, B., Li, C. R., Miyauchi, Y., Kuwaki, O., & Shiratori, S. (2006a). Formation of novel 2D polymer nanowebs via electrospinning. *Nanotechnology, 17*, 3685–3691.

Elbakry, A., Zaky, A., Liebkl, R., Rachel, R., Goepferich, A., & Breunig, M. (2009). Layer-by-layer assembled gold nanoparticles for siRNA delivery. *Nano Letters, 9*, 2059–2064.

Fakhry, A., Schneider, G. B., Zaharias, R., & Senel, S. (2004). Chitosan supports the initial attachment and spreading of osteoblasts preferentially over fibroblasts. *Biomaterials, 25*, 2075–2079.

Geng, X., Kwon, O.-H., & Jang, J. (2005). Electrospinning of chitosan dissolved in concentrated acetic acid solution. *Biomaterials, 26*, 5427–5432.

Heinemann, C., Heinemann, S., Bernhardt, A., Worch, H., & Hanke, T. (2008). Novel textile chitosan scaffolds promote spreading, proliferation, and differentiation of osteoblasts. *Biomacromolecules, 9*, 2913–2920.

Heinemann, C., Heinemann, S., Lode, A., Bernhardt, A., Worch, H., & Hanke, T. (2009). In vitro evaluation of textile chitosan scaffolds for tissue engineering using human bone marrow stromal cells. *Biomacromolecules, 10*, 1305–1310.

Ingrosso, C., Petrella, A., Curri, M. L., Striccoli, M., Cosma, P., Cozzoli, P. D., et al. (2006). Photoelectrochemical properties of hybrid junctions based on zinc phthalocyanine and semiconducting colloidal nanocrystals. *Electrochimica Acta, 51*, 5120–5124.

Ji, Y., Ghosh, K., Shu, X. Z., Li, B. Q., Sokolov, J. C., Prestwich, G. D., et al. (2006). Electrospun three-dimensional hyaluronic acid nanofibrous scaffolds. *Biomaterials, 27*, 3782–3792.

Kim, W. T., Chung, H., Shin, I. S., Yam, K. L., & Chung, D. H. (2008). Characterization of calcium alginate and chitosan-treated calcium alginate gel beads entrapping allyl isothiocyanate. *Carbohydrate Polymers, 71*, 566–573.

Kim, J. S., Rieter, W. J., Taylor, K. M. L., An, H., Lin, W. L., & Lin, W. B. (2007). Self-assembled hybrid nanoparticles for cancer-specific multimodal imaging. *Journal of the American Chemical Society, 129*, 8962–8963.

Kokubo, H., Ding, B., Naka, T., Tsuchihira, H., & Shiratori, S. (2007). Multi-core cable-like TiO_2 nanofibrous membranes for dye-sensitized solar cells. *Nanotechnology, 18*.

Kurita, K. (2006). Chitin and chitosan: Functional biopolymers from marine crustaceans. *Marine Biotechnology, 8*, 203–226.

Laurent, D., & Schlenoff, J. B. (1997). Multilayer assemblies of redox polyelectrolytes. *Langmuir, 13*, 1552–1557.

Lee, S. W., Kim, B. S., Chen, S., Shao-Horn, Y., & Hammond, P. T. (2009). Layer-by-layer assembly of all carbon nanotube ultrathin films for electrochemical applications. *Journal of the American Chemical Society, 131*, 671–679.

Lee, S. H., Kumar, J., & Tripathy, S. K. (2000). Thin film optical sensors employing polyelectrolyte assembly. *Langmuir, 16*, 10482–10489.

Lu, J. W., Zhu, Y. L., Guo, Z. X., Hu, P., & Yu, J. (2006). Electrospinning of sodium alginate with poly(ethylene oxide). *Polymer, 47*, 8026–8031.

Ogawa, T., Ding, B., Sone, Y., & Shiratori, S. (2007). Super-hydrophobic surfaces of layer-by-layer structured film-coated electrospun nanofibrous membranes. *Nanotechnology, 18*.

Pasparakis, G., & Bouropoulos, N. (2006). Swelling studies and in vitro release of verapamil from calcium alginate and calcium alginate–chitosan beads. *International Journal of Pharmaceutics, 323*, 34–42.

Ravi Kumar, M. N. V. (2000). A review of chitin and chitosan applications. *Reactive and Functional Polymers, 46*, 1–27.

Rowley, J. A., Madlambayan, G., & Mooney, D. J. (1999). Alginate hydrogels as synthetic extracellular matrix materials. *Biomaterials, 20*, 45–53.

Sennerby, L., Röstiund, T., Albrektsson, B., & Albrektsson, T. (1987). Acute tissue reactions to potassium alginate with and without colour/flavour additives. *Biomaterials, 8*, 49–52.

Shiratori, S. S., & Rubner, M. F. (2000). pH-dependent thickness behavior of sequentially adsorbed layers of weak polyelectrolytes. *Macromolecules, 33*, 4213–4219.

Yang, X. C., Chen, X. N., & Wang, H. J. (2009). Acceleration of osteogenic differentiation of preosteoblastic cells by chitosan containing nanofibrous scaffolds. *Biomacromolecules, 10*, 2772–2778.

Yi, H. M., Wu, L. Q., Bentley, W. E., Ghodssi, R., Rubloff, G. W., Culver, J. N., et al. (2005). Biofabrication with chitosan. *Biomacromolecules, 6*, 2881–2894.

Zhang, L. B., Chen, H., Sun, J. Q., & Shen, J. C. (2007). Layer-by-layer deposition of poly(diallyldimethylammonium chloride) and sodium silicate multilayers on silica-sphere-coated substrate-facile method to prepare a superhydrophobic surface. *Chemistry of Materials, 19*, 948–953.

Zhang, Y. Z., Lim, C. T., Ramakrishna, S., & Huang, Z. M. (2005). Recent development of polymer nanofibers for biomedical and biotechnological applications. *Journal of Materials Science – Materials in Medicine, 16*, 933–946.